

Significance of compact layers on DSSCs performance of chemically deposited TiO₂-based Dye-sensitized solar cells

Vijaykumar S. Jadhav, Sambhaji S. Bhande,^a Kailas K. Tehare,^a Sanjay L Gaikwad, Rajaram S. Mane^{a,*}

^aCentre for Nanomaterials & Energy Devices, School of Physical Sciences, SRTM University, 431606, Nanded, India

ABSTRACT

Abstract : We report on beneficial effects of compact TiO₂ blocking layers on the performance of dye-sensitized solar cells (DSSCs) fabricated using chemically deposited TiO₂ nanorice structures. In presence of compact layers, short circuit current density was improved to 11.5 mA/cm². The investigation of charge transfer kinetics in the system showed that charge transfer resistance reduced considerably in presence of compact layers indicating effective coupling and good contact between the layers.

Keywords: Compact layers; Structural Elucidation; Electrical properties; Electrodeposition

Date of Submission: 21 September 2015



Date of Accepted: 03 October 2015

I. Introduction

Dye-sensitized solar cell (DSSC) characterized by low cost, high efficiency, and capability for environmental protection. It shows considerable potential as a new generation commercial solar cell.[1,2] Recently, over 11% power conversion efficiency have been achieved;[3] however this value is still lower than that of conventional silicon solar cells. Accordingly, various investigations have been undertaken to enhance the power conversion efficiency (η %) of DSSC. The porous TiO₂ layer essentially serves the purpose of collecting and transporting photoelectrons injected by the photo-excited dye *via* the TiO₂ conduction band to the conducting substrate, and then to the external circuit. However, interfacial contact between TiO₂ and FTO contains several defects due to lattice mismatch which can lead to form few voids and decrease the short circuit current density (J_{sc}). [4-6] Direct contact between fluorine-tin-oxide (FTO) substrate and electrolyte interface can potentially increase recombination. [7] The interaction of redox couple with the conductive substrate results in recombination of electron arriving from the conduction band of TiO₂. The use of a compact layer between the FTO and nanocrystalline TiO₂ has been actively studied in literature. [8-10] Presence of such a compact layer improves the adhesion of the TiO₂ to the FTO and provides a larger TiO₂/TCO contact area and more effective electron transfer from the TiO₂ to the FTO by preventing the electron recombination process, which occurs in the interface between the redox electrolyte and the FTO surface.

In addition, there are many factors limiting the performance of the DSSC, as such the absorption of a large fraction of the incident solar light by the photoactive layer of dye-sensitized photoanode and the use of wide light absorption bands and co-sensitization of the photoanode are important for achieving high efficiency.[11,12] On the other hand, the conventional semiconductor photoanode, which is composed of small nanoparticles with size of 10-30 nm, provides large surface area for dye adsorption, however, is transparent to the solar light and could not effectively utilize the incident light.[13] Incorporating large particles or pores in the nanocrystalline photoanode or depositing a layer of large particles on the nanocrystalline photoanode to enhance the light scattering and light absorption in the photoanode is investigated experimentally [14-17] and theoretically[18-21] for enhancing power conversion efficiency of DSSC.

In continuation of our study regarding to TiO₂ nanostructures based working electrode. [22-25] In the present investigation the use of different TiO₂ compact layers by using a cost effective spray pyrolysis and sol-gel method at FTO/TiO₂ nanorice (prepared by a wet-chemical method) interface, which plays important role of creating energy barrier between FTO substrate and porous TiO₂ nanostructure electrode. Furthermore, a four micron thick nanorice layer of rutile TiO₂ is deposited on it using wet chemical method. This layer composed of nanorice and micro plates, acts as a scattering layer for light entering into it providing a longer path to travel. Combining these two different strategies power conversion efficiency of rutile TiO₂ nanorice-based DSSC has been increased which is investigated in depth. It is noteworthy that for better lattice correlation both compact layer and rutile TiO₂ nanorice synthesis have been carried out from the same precursor solution i.e. TiCl₄ unlike in routine TiO₂- based DSSC where sprayed TiO₂ and TiO₂ dye-sol, respectively, are considered.

II. Experimental details

Prior to deposition of TiO₂ nanostructure the FTO substrate was cleaned with detergent and then ultrasonically cleaned in acetone and methanol for 20 minutes followed by rinsing in deionized water, and subsequently dried in a flowing nitrogen gas. In the next step, solution of TiCl₄ was firstly converted to 1 M solution by adding the calculated volume of HCl, triply-distilled water and TiCl₄ solution. This mixture was then kept at 273 K, for 30 minutes, the yellow color of solution was turned to colorless. This prepared solution was used as our stock solution for both spray and spin coating operations. The compact layer of TiO₂ nanoparticles was obtained using a spray pyrolysis method. The FTO-glass substrates (2.5 x 2.5 x 0.15 cm³) were mounted on a heating plate placed 300 mm below an atomizer with a glass nozzle. The substrate was kept at temperatures 723 K. The suspension of 0.1 M TiCl₄ (15 ml) was sprayed with spraying and gas flow rates of 2 ml/min and 10 L/min, respectively. The spin coating of TiO₂ nanoparticles *via* spin coater was obtained with 0.1 M TiCl₄ mixed with 0.1 M thiorea milky indicated the formation of Ti (OH)₂ nanoparticles due to a process of oxidation. This faint-milky gel was spin-coated on FTO-glass at 2000 rpm for 5 minutes and then annealed at 723 K. In the final step, these above prepared compact layers of TiO₂ were used as base layers for synthesizing porous TiO₂ nanorice using a procedure reported elsewhere. [26] In nutshell, TiCl₄ and 0.1 M thiorea were mixed in equal proportion. One TiO₂ compact layer free FTO electrode was also placed for comparing obtained results. Reaction was allowed to perform at 338 K for 6h. Whitish non-transparent samples were obtained. The TiCl₄ treatment consisted of soaking the prepared films in 0.2 M aqueous TiCl₄ for 50 min, followed by sintering at 723 K for 30 min was carried out on all electrodes. These electrodes were dipped in N719 dye for 20 hrs and used in DSSC after rinsing with acetonitrile and drying at room temperature. The redox electrolyte, consisting of 0.6 M 1, 2-dimethyl-3-hexyl imidazolium iodide, 0.2 M LiI, 40 mM I₂, and 0.2 M *tert*-butyl pyridine in acetonitrile, was introduced into the cell through one of the two small holes drilled in the counter electrode.

III. Results and Discussion

3.1. Device form and structural analysis

Fig. 1 (a) shows the XRD spectra of TiO₂ electrodes of pristine and other two were for compact TiO₂ layered.

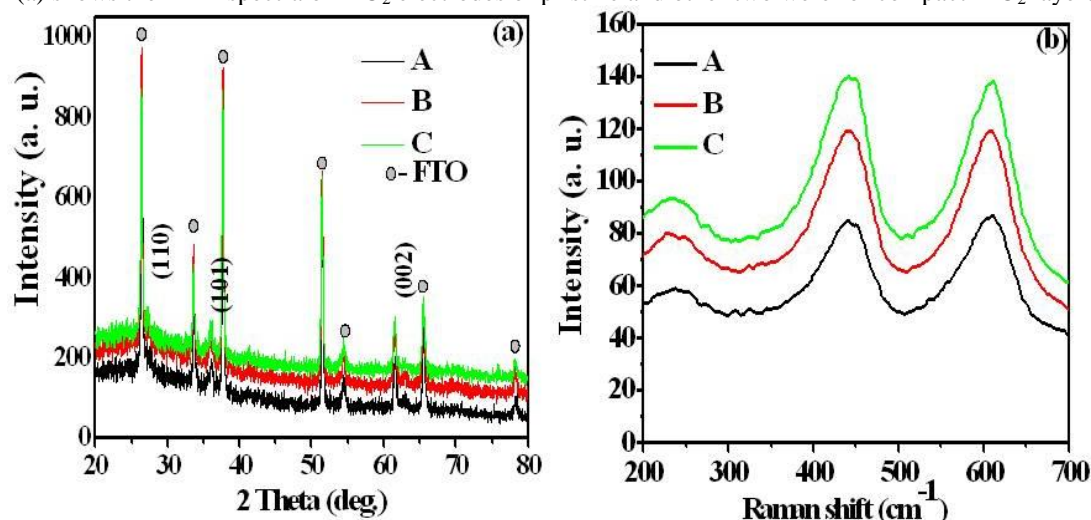


Figure 1. (a) The X-ray diffraction pattern and Raman analysis, confirming the rutile nature of TiO₂ in all three cases of TiO₂ synthesis. (b) Raman analysis of all three samples tested

The rutile form of all three electrodes was confirmed as the characteristic peaks for other forms including anatase and brookite were completely absent. The (111) and (002) diffraction peaks are nearly of same intensity in comparison with (101) [27] when compared with the standard rutile TiO₂ form (JCPDF No. 87-0920), indicating that there is no anisotropic growth other than rutile. Some of the peaks other than these peaks represent FTO. The average grain size was obtained by averaging *D* (estimated grain size) for different strong and weak intensity peaks in the XRD spectrum obtained software provided and was 5 nm. To support this conclusion Raman spectrums obtained from the room temperature Raman spectroscopy carried out on these TiO₂ electrodes are presented in Figure 1 (b). In all electrodes three major peaks at 238, 240 and 609 cm⁻¹ correspond to B1g, Eg and A1g as active modes were identified and were closely match with reported values of Lee *et. al.* indicating the formation of rutile. For anatase phase Raman intensity locations are at 515 and 640 cm⁻¹ [28] supporting that both compact and porous layers of TiO₂ are of rutile form.

3.2. Morphological evolution and optical absorption studies

Figure 2 (a, b and c) shows the surfaces of sprayed and spin-coated compact layers in addition to wet-chemically grown porous TiO₂ nanorice.

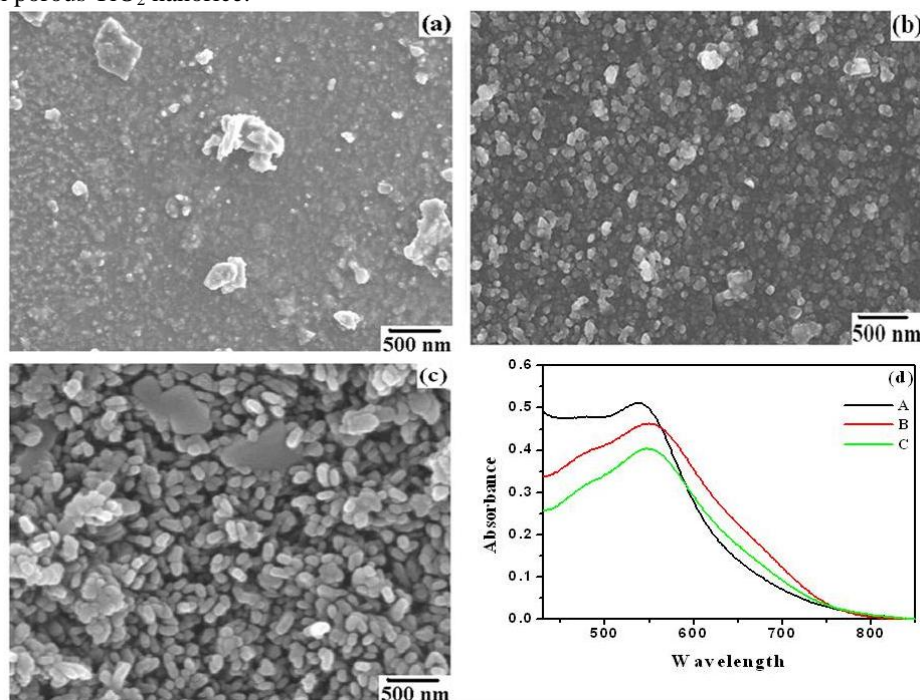


Figure 2. SEM images of (a) spray pyrolysis TiO₂ compact layer, (b) Spin coated TiO₂ (c) Chemical bath deposited Porous TiO₂ and (d) Uv-Visible spectrum of as synthesis samples

Surface architecture of sprayed compact layer [Fig. 2a] was made up of dispersed nanoislands of few nanometers in dimension with unavoidable relatively big irregular structures. In contrast to this, uniformly distributed nanospheres of TiO₂ were seen in spin-coated compact layer [Fig. 2b]. It was presumed that due to regular arrangement and smaller particle size with large surface area the compact layer of spin-coated TiO₂ might favor more interfacial contacts with porous TiO₂ nanorice. Fig. 2c is the surface of wet-chemically grown TiO₂ nanorice. On both compact layers there was no significant change in TiO₂ nanorice architecture. A porous TiO₂ nature with nanorice morphology was believed to increase the absorption path length of photons, thus light-scattering can be enhanced to increase the light harvesting yield [29, 30] and thereby, high power conversion efficiency. Fig. 2 (d) shows the UV-vis optical absorption spectra of pristine and compact layers supported TiO₂ nanorice loaded with N719 dye for 20 h. Compared to compact layers-supported TiO₂ nanorice electrodes pristine electrode shows at 550 nm wavelength. Due to increase in overall TiO₂ a slight red-shift was confirmed. Due smaller in sizes dye adsorption in sprayed compact layer supported TiO₂ electrode is weak compared with spin-coated.

3.3. Impact of compact layers on cell performance

The porous nature of thin films provides high surface area but also provides the path for redox electrolyte to penetrate through it, making a direct contact with bare working electrode (e.g., FTO, ITO). At these bare sites, the potential is thermodynamically favorable for the reduction of oxidative species like I₃⁻ resulting in low performance of the cell.[31] Controlling the recombination's across conducting electrode/metal oxide interface is vital to enhance the energy conversion from solar to electric in dye sensitized solar cells. In Fig. 3 (a) shows variation in current density-applied voltage plots correspond to pristine and compact layers-supported TiO₂ electrodes.

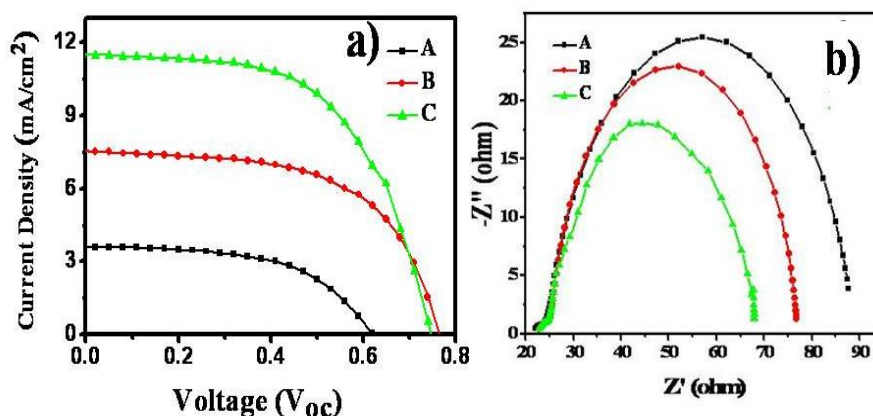


Figure 3. (a) I-V characteristics Curve (b) Nyquist plots of all three cells tested.

Pristine TiO₂ nanostructure electrode revealed inferior enclosed area compared with compact-layers supported electrodes indicating that infiltration of dye molecules and electrolyte has been effectively blocked by compact layers. Pristine, spin and sprayed-supported TiO₂ electrodes showed series resistances 21.37, 21.36 to 22.38 Ω cm⁻², respectively tabulated in table 1.

Table 1. Parameters obtained by J-V and EIS analysis of A, B and C

Sample	J _{sc} (mA/cm ²)	V _{oc} (V)	FF	Eff. (%)	R _s (Ω-cm)	R ₁ (Ω-cm)	R ₂ (Ω-cm)
A	4.14	0.75	0.52	1.62	21.37	3.58	63.91
B	7.55	0.76	0.63	3.66	21.36	3.15	51.37
C	11.49	0.74	0.58	4.96	22.38	3.08	42.70

It is interesting to note that the open circuit voltage (V_{oc}) in all three electrodes tested showed approximately same value (variation ~ ± 0.01 V), however current density was drastically increased from 4.14 to 11.49 mA/cm² indicating that charge transport in compact layers-supported electrodes is easier and faster than in pristine TiO₂ electrode. It is mandatory to mention here that the current density is mainly influenced by dye loading and secondly by charge recombination at the working electrode.[32,33] Increased fill factor (reduced charge transfer resistance across FTO/TiO₂) from 0.52 to 0.58 followed by current density enhanced power conversion efficiency 1.62 to about 5% (demonstrated in table 1), which is remarkable. In nutshell, constructive pathway to facilitate effective electron transfer can be provided in presence of compact layer by increasing overall conversion efficiency.

To support these observations electrochemical impedance spectroscopy measurements for these three electrodes were carried out under open circuit voltage and light illumination. The EIS spectra revealed two semicircles one at higher frequency and second at lower. The semicircle in high frequency represents the interface between counter electrode (platinum) and electrolyte whereas the semicircle in low frequency refers to the interface between titanium dioxide/dye and electrolyte. The obtained Nyquist plots and the equivalent circuits employed for their fitting are displayed in Figure 3 (b) and in inset, respectively. A clear difference in Nyquist plots obtained for pristine and compact layer-supported TiO₂ electrodes was seen. High frequency semicircle in all cases is smaller compared to intermediate semicircle indicating that the charge transfer resistance of the working electrode-electrolyte interface is much slower than at the counter electrode interface; i.e., the reduced dye gets electrons or regenerated by the

Conversion of 3I⁻ to I₃⁻ ions. From the above perceptions, the TiO₂ nanorice electrode with spin-coated compact layer offered the least R_{ct} which was considered as the pre-eminent system to offer high efficiency in correlation with the J-V characteristics. This is because of the compact layer physically blocks the reaction of

the photo-injected electrons and the I_3^- ions at the FTO/electrolyte interface. Such a compact film cannot only separate the electrolyte from the substrate, but also improve the adhesion of the porous TiO_2 film. The compact film also refers to the blocking film or the passivating layer in the literatures. [34] Therefore, controlling the interface between the FTO and TiO_2 nanorice electrode can be essential for the formation of efficient DSSCs.

IV. Conclusions

The effect of the compact layer prepared by two different methods was investigated for the performance of DSSCs. The compact TiO_2 film with few nanometer grains as a compact layer not only improve adherence of TiO_2 to FTO but also provides a larger TiO_2 /FTO contact area and effectively reduce the electron recombination by minimizing the direct contact between the redox electrolyte and the conductive FTO surface. It is confirmed from the obtained results that the compact film with high surface area is preferable for high current density, in device performance. The current density increased from 4.14 to 11.496 mA/cm² with spin coated compact layer, where as the more flattened compact layer with sprayed TiO_2 showed comparatively lower performance due to higher flattened surface area. It was confirmed from the impedance analysis, where charge transport resistance in case of spin coated compact layer based DSSC showed least resistance and hence supports long life time for electron transport.

V. Acknowledgement

Thanks to University Grant Commission, New Delhi, India for providing financial assistance through a research project: 41-844/2012(SR).

Notes and references

- [1] B. Oregan and M. Gratzel, *Nature* 1991, **353**, 737.
- [2] M. K. Nazeeruddin, A. Kay, I. Rodicio, R. Humphrybaker, E. Muller, P. Liska, N. Vlachopoulos, and M. Gratzel, *J. Am. Chem. Soc.* 1993, **115**, 6382.
- [3] M. Gratzel, *Nature* 2001, **414**, 338.
- [4] K. Srinivas, K. Yesudas, K. Bhanuprakash, V. Jayathirtha Rao, and L. Giribabu, *J. Phys. Chem. C* 2009, **113**, 20117.
- [5] G. D. Sharma, P. Suresha and J. A. Mikroyannidis, *Synth. Met.* 2010, **160**, 1427.
- [6] H. Yu, S. Q. Zhang, H. J. Zhao, G. Will and P. Liu, *Electrochim. Acta* 2009, **54**, 1319.
- [7] B. C. O'Regan, J. R. Durrant, P. M. Sommeling and N. J. Bakker, *J. Phys. Chem. C* 2007, **111**, 14001.
- [8] B. Peng, G. Jungmann, C. Jager, D. Haarer, H-W. Schmidt and M. Thelakkat, *Coordin. Chem. Rev.* 2004, **248**, 1479.
- [9] H. Yu, S. Zhang, H. Zhao, G. Will and P. Liu, *Electrochim. Acta* 2009, **54**, 1319.
- [10] J. Shi, J. Liang, S. Peng, W. Xu, J. Pei and J. Chen, *Sol. Stat. Sci.* 2009, **11**, 433.
- [11] G. Rothenberger, P. Comte and M. Gratzel, *Sol. Eng. Mat. Sol. Cells* 1999, **58**, 321.
- [12] M. Gratzel, *J. Photochem. Photobio. C- Photochem. Rev.* 2003, **4**, 145.
- [13] B. Tan, and Y.Y. Wu, *J. Phys. Chem. B* 2006, **110**, 15932.
- [14] H. J. Koo, Y. J. Kim, Y. H. Lee, W. I. Lee, K. Kim, and N. G. Park, *Adv. Mat.* 2008, **20**, 195.
- [15] Y. Chiba, A. Islam, R. Komiya, N. Koide, and L. Y. Han, *Appl. Phys. Lett.* 2006, **88**, 223505.
- [16] S. Hore, P. Nitz, C. Vetter, C. Prahl, M. Niggemann, and R. Kern, *Chem. Commun.* 2005, **15**, 2011.
- [17] Z. S. Wang, H. Kawauchi, T. Kashima, and H. Arakawa, *Coord. Chem. Rev.* 2004, **248**, 1381.
- [18] A. Usami, *Chem. Phys. Lett.* 1997, **277**, 105.
- [19] Y. Tachibana, K. Hara, K. Sayama and H. Arakawa, *Chem. Mat.* 2002, **14**, 2527.
- [20] J. Ferber and J. Luther, *Sol. Eng. Mat. Sol. Cells* 1998, **54**, 265.
- [21] R. Stangl, J. Ferber and J. Luther, *Sol. Eng. Mat. Sol. Cells* 1998, **54**, 255.
- [22] K. K. Tehare, M. K. Zate, S. S. Bhande, S. A. Patil, S. L. Gaikwad, S-J. Yoon, R. S. Mane, S-H. Lee and S-H. Han, *J. Mater. Chem. A*, 2014, **2**, 478.
- [23] S. S. Bhande, D. V. Shinde, K. K. Tehare, S. A. Patil, R. S. Mane, Mu. Naushad, Z.A Alothman, K.N. Hui, S-H Han, *J. Photochem. and Photobio. A: Chemistry*, 2014, **295**, 64.
- [24] S.A. Patil, D.V. Shinde, D-Y. Ahn, D.V. Patil, K. K. Tehare, V. V. Jadhav, J-K Lee, R.S. Mane, N. K. Shrestha and S-H Han, *J. Mater. Chem. A*, 2014, **2**, 13519.
- [25] K. K. Tehare, R. S. Mane and S-H Han, *SRTMU's Res. J. Sci.* 2012, **1(1)**, 1.
- [26] P. Liu, W. Cai, M. Fang, Z. Li, H. Zeng, J. Hu, X. Luo, and W. Jing, *Nanotechnology* 2009, **20**, 285707.
- [27] G.-W. Lee, S. B. Ambade, Y.-J. Cho, R. S. Mane, V. Shashikala, J. Yadav, R. S. Gaikwad, S-H. Lee, K-D. Jung, S-H. Han, and O-S Joo, *Nanotechnology* 2010, **21**, 105603.
- [28] W. F. Zhang, Y. L. He, M. S. Zhang, Z. Yin, and Q. Chen, *J. Appl. Phys. D* 2000, **33**, 912.
- [29] S. H. Kang, J-Y. Kim, H. S. Kim, H-D. Koh, J-S. Lee, and Y-E. Sung, *J. Photochem. Photobiol. A Chem.* 2008, **200**, 294.
- [30] S. Hore, C. Vetter, R. Kern, H. Smit, and A. Hinsch, *Sol. Eng. Mat. Sol. Cells* 2006, **90**, 1176.
- [31] H. Yu, S. Zhang, H. Zhao, G. Will and P. Liu, *Electrochim. Acta* 2009, **54**, 1319.
- [32] A. N. M. Green, E. Palomares, S. A. Haque, J. M. Kroon, and J. R. Durrant, *J. Phys. Chem. B* 2005, **109**, 12525.
- [33] S. Nakade, T. Kanzaki, W. Kubo, T. Kitamura, Y. Wada and S. Yanagida, *J. Phys. Chem. B*, 2005, **109**, 3480.
- [34] J. A. Jeong, and H. K. Kim, *Sol. Eng. Mater. Sol. Cells* 2011, **95**, 344.